Transition of Crystal Growth as a Result of Changing Polymer States in Ultrathin Poly(ethylene oxide)/Poly(methyl methacrylate) Blend Films with Thickness of <3 nm

Mingtai Wang,* Hans-Georg Braun,* and Evelyn Meyer

Institute of Polymer Research Dresden, Hohe Strasse 6, D-01069 Dresden, Germany

Received October 20, 2003; Revised Manuscript Received November 10, 2003

ABSTRACT: The transition of crystal growth is revealed in ultrathin poly(ethylene oxide)/poly(methyl methacrylate) (PEO/PMMA) blend films (film thickness $D < 3$ nm) as the crystallization condition changes from vacuum to humidity. The PEO crystallizes into a fractal-like branched structure in a vacuum from a state mixed with PMMA, but in humidity into one reminiscent of dense branching morphology (DBM). The crystal lamellae in both conditions orient flat-on, but the DBM-like structure is much thicker and wider, indicating a crystallization more close to equilibrium. Results show that as a PEO/PMMA blend film is exposed to humidity, PEO chains demix with PMMA and segregate on a PMMA layer before or during crystallization. The crystal growth transition is attributed to the change in the factors that dominate the crystal growth at crystal growth fronts, that is, the kinetic and surface tension effects, as a result of changing the polymer states in the blend films. The crystal growth of the demixed PEO on the PMMA layer is dominated by a strong surface tension effect, while crystal growth of PEO in a blend/mixed state is dominated by either a kinetic effect or a weak surface tension effect depending on the film composition. The compositional dependence of the crystal growth in humidity is also elucidated on the basis of the changing of polymer states in the films.

Introduction

As a typical confined geometry system, special enthalpic and entropic effects at the polymer/substrate interface cause the mobility,[1] crystallinity,[2] orientation,[3,4] and dewetting[5] of polymer chains in ultrathin films (film thickness $D < 100$ nm) to depend on film thickness. Even though contradictory results are reported on the chain mobility,[1] it seems that the glass transition temperature T_g of polymers in ultrathin films can be either lowered or increased, depending on the interfacial interactions.[6] On the other hand, the crystallization in ultrathin films has received considerable attention in recent years. The studies in this field may mainly be classified into three groups according to the film thickness used, $D > 20$ nm,[2,3,7−10] $5 < D < 20$ nm,[11,12] and $D < 5$ nm,[13−19] and one general conclusion is that the crystalline morphology in ultrathin films changes greatly with the film thickness. As found in poly(ethylene oxide) (PEO) films by Frank et al., the growth of lamellar crystals that prefer a flat-on orientation on substrate is exclusive in the films with thickness in the 15−300 nm range,[7−9] which is reminiscent of the faceted growth of PEO crystal lamellae in films with thickness on order of tens of micrometers;[20,21] however, the crystal growth exhibits a dendritic habit when PEO films have $D < 15$ nm.[8] Miyaji et al.[11,12] reported the crystalline morphology in ultrathin isotactic polystyrene (it-PS) films with $5 < D < 20$ nm. Their results[11] show that the films with $D < 20$ nm exhibit branched crystalline morphologies which turn, with thickness decreasing to below 10 nm, from a compact seaweed structure into one typically formed by a diffusion-limited aggregation (DLA) process,[22] and the width of crystalline branches has a dependence on the inverse of film thickness. As for the crystallization when $D < 5$ nm, the branched structures due to nonequilibrium crystallization by the DLA process are always the case in the films, for example, of poly(ethylene terephthalate)[13,14] and PEO.[15−19] The branches are generally crystal lamellae viewed flat-on with polymer chains folded by a stem length of 7−13 nm and oriented normal to the substrate surface[15−19] or inclining a small angle from the basal plane normal.[13] Interestingly, for chain (e.g., PEO) orientation along the surface normal direction crystallization remains possible even if the lamellar thickness excesses the film thickness,[8] but as polymer chains favor the orientation in the direction parallel to film plane crystal growth may be inhibited as D decreases to below a certain threshold value, for example, 15 nm in poly(di-*n*-hexylsilane) (PD6S) films.[2,3] Obviously, as the thickness of films reduces down to $D < 20$ nm, the crystalline morphologies formed in them become quite different from the bulk crystallization that normally results in spherulitic crystalline texture.

Since the chain mobility can be changed by the interfacial effects in ultrathin films, the crystal growth kinetics that is strongly related to the transport property of chains is consequently altered by film thickness. The decrease in film thickness normally reduces the crystallization rate,[2,7−12,23] mainly by reducing the mobility of polymer chains.[7−12,23] The crystal growth rate decreases with reducing the thickness of PEO films;[7−10] this was presumably due to the increased T_g of the confined PEO chains and the concomitant reduction of molecular mobility.[8,9] In it-PS films with D down from 500 to 20 nm, the dependence of crystal growth rate $G_{(d)}$ on the film thickness D was found to follow the relationship of $G_{(d)} = G_{(\infty)}(1 - C/D)$, where $G_{(\infty)}$ was the crystal growth rate in bulk state and C was a constant of 6 nm that was independent of the crystallization temperature (T_c), molecular weight of the polymer, and substrate material and was interpreted

* Corresponding authors: Tel 0049-351-4658548; Fax 0049-351-4658284; e-mail mingtaiwang@hotmail.com (Wang), braun@ipfdd.de (Braun).

10.1021/ma0355812 CCC: $27.50
Published on Web 12/18/2003

as the tube diameter in the reptation model of polymer dynamics.[23] It was regarded that the decrease of the crystal growth rate with decreasing the film thickness was due to the reduction of chain mobility as a result of the reduction in the reptation tube diameter near substrate. As reported in the it-PS films of $D < 20$ nm,[11] the crystal growth rate decreases with film thickness ($D > 8$ nm) according to the relationship $G_{(d)} \sim (1 - C/D)$. While the crystal growth rate also decreases with film thickness as it is below the value of 8 nm, which is the thickness of the it-PS crystal lamellae, the relationship $G_{(d)} \sim (1 - C/D)$ does not hold any longer, and the reduction in crystal growth rate is attributed to the increased diffusion path of polymer chains in the thinner films; however, the crystal growth rate remains unchanged in the films of $D < 5$ nm.

Recently, a lattice model has been proposed by Reiter and Sommer[17] for the crystal growth in two dimensions, where the polymer chains are considered as the smallest units in crystallization process and the crystal growth is diffusion-controlled. During the crystal growth in this model the attachment of polymer chains proceeds by a multistep process, namely, a chain deposits first on a crystal surface with various degrees of internal order, then it tries to get a better order afterward within the crystal by relaxation or reorganization. Their simulation has provided a successful algorithmic understanding of the crystalline morphologies experimentally formed in PEO monolayers ($D < 5$ nm).[15,16] Accordingly, the lamellar dimensions (thickness and width) are related to the kinetics of chain deposition at crystal growth fronts. Our results[18] show that a lowered chain deposition rate (or sticking probability) at crystal growth fronts, namely, a reduced crystal growth rate, as a result of the reduction in polymer concentration in the diffusion field, makes newly deposited chains have a high probability to rearrange to a state near equilibrium and occupy the highest number of nearest neighbors when they finally stick to the fronts, giving wider and thicker crystal branches. In isothermal crystallization of PEO monolayer,[15,16] the thickness and width of crystal lamellae were observed to increase with T_c. When a crystal grows slowly (low undercooling), the molecules attached to the crystal have more time to relax toward the fully extended form of lowest free energy by rearrangements at the crystal surface.[16] Moreover, the width of crystal lamellae is directly related to the average diffusion path of a chain before it gets trapped in the crystal phase. The increase in the effective diffusion path, which will inevitably reduce the chain deposition rate at crystal growth fronts, was regarded to be responsible for the coarsening of crystal lamellae with increasing T_c in PEO films[16,17] and with decreasing the film thickness in the isothermal crystallization in it-PS films.[11] From these studies of the films with $D < 5$ nm, a common conclusion can be drawn; that is, a lowered chain deposition rate at crystal growth fronts favors the growth of wider and thicker crystal lamellae.

During the passed several decades, the polymer crystallization has been extensively studied, and many experiments and theories, sometimes controversial, have been published.[24,25] In bulk state polymers normally crystallize into spherulites. In experiments one typical feature in spherulite formation is the linear growth of spherulite radius vs time.[26−28] In PEO films with thickness in the range of 40 nm−1 μm, the crystals have a linear growth feature.[10] But in the thin film of poly(hydroxybutyrate-*co*-valerate) copolymer the crystal lamellae were not observed to grow by a constant rate, therefore giving some controversial topics in the field of existing polymer crystallization theories.[27] As found by Frank et al.[2] in ultrathin PD6S films, the crystal growth is 3-dimensional in films of $D > 22$ nm but changes to 1-dimensional as $D < 15$ nm. However, in PEO films of $20 < D < 300$ nm the crystal growth (2- or 3-dimensional) is not altered by film thickness.[8] Analysis of the crystallization kinetics, on the basis of Hoffman−Weeks extrapolation, the Gibbs−Thomson equation, and the Hoffman−Lauritzen theory, shows that the crystallization in PEO films with $D > 15$ nm is governed by the same laws as the bulk crystallization.[9] It is interesting that in the it-PS films of $5 < D < 20$ nm the crystals also grow linearly.[11] Unfortunately, to our knowledge, we are lacking the data on the crystal growth kinetics in the films with $D < 5$ nm. Since the experimental studies on crystallization kinetics in the films with $D < 20$ nm are very limited, whether the experimental and theoretical results obtained in bulk crystallization apply to such thin films is still far from conclusion and needs systematical investigations.

So far, the studies on the crystallization in films with $D < 5$ nm are mainly confined in homopolymer films.[13−18] However, many practical applications involve use of polymer blends, which is an economical way to get materials with defined functions. As a model blend system, the bulk blends consisting of PEO and poly(methyl methacrylate) (PMMA) have been intensively studied[28] (also see the references cited in ref 19). However, aside from our previous report,[19] there have been few investigations on ultrathin PEO/PMMA blend films, in particular, with D of a few nanometers.[29] The crystallization in polymer blend films would be more complex than homopolymer ones due to film composition, film structure, and possible interaction between blend components. Our previous work[19] shows the crystalline structure in ultrathin blend films consisting of PEO and PMMA with a thickness comparable to the radius of gyration R_g of polymer, and a fractal-like branched structure results in a vacuum in those blend films due to the heterogeneously nucleated crystallization of PEO by a DLA process. The crystalline branches formed in the blend films are crystal lamellae viewed flat-on on substrate. Increasing PMMA content generally leads to a stronger retardation effect of PMMA on PEO crystallization. As compared to bulk crystallization, the retardation effect of PMMA is dramatically enhanced by constrained geometry. This result agrees with that the effective interdiffusion coefficients are dramatically decreased at the distance of $3R_g$ from substrate surface.[30] When PMMA content is high (ca. $\geq$40%), the retardation effect dominates the crystal growth process, leading to crystal lamellae thicker than those formed in pure PEO films. Opposite to the case of a high PMMA content, PEO crystallization is much farther away from equilibrium in the films with a rather low PMMA content, for example, in 90/10 (= PEO/PMMA) and 75/25 films. Another remarkable feature in the PEO/PMMA blend films crystallized in a vacuum is that the width of crystal lamellae (ca. 0.2 μm) is independent of the film composition. However, as the PEO/PMMA blend films crystallized in humidity, the crystalline structures became quite different in that they were much wider and thicker than the fractal-like ones. Different from the crystallization in a vacuum,

both the thickness and width of the crystalline branches were dependent on PMMA content in the humidity crystallization. Results showed that the different crystal growth habits in a vacuum and humidity were related to the change in polymer states in the PEO/PMMA films, as summarized in this study.

Experimental Section

Poly(ethylene glycol) standard ($M_w = 6000$, $M_w/M_n = 1.03$) from Fluka and PMMA standard ($M_w = 4200$, $M_w/M_n = 1.06$) from Polymer Standards Services (PSS, Germany) were used as received. All the PEO used in this study refers to this poly(ethylene glycol) standard, except for the shorter PEO specified in the text. The PEO chains were terminated by OH at both ends (i.e., $HO-(CH_2CH_2O)_n-H$), as known from the data provided by the manufacturer. The radius of gyration, R_g, of the PEO and PMMA was 3.30 and 1.77 nm, respectively. The PEO/PMMA blend films were dip-coated from chloroform solutions (totally 1 mg/mL) at an average lifting rate of 1.90 mm/s on Au films (100 nm thick) supported on glass slides that were covered prior by a 3 nm Cr adhesive layer, and ellipsometric measurements showed that the as-coated films had a thickness of 2−3.0 nm when a refractive index of 1.5 was given to the polymer layers. For $D \leq R_g$ of the longest component (PEO), the films were in an extremely constrained state.[19] For such thin films, heterogeneous nucleation is necessarily important to initiate crystallization.[2]

The films for the observations by means of scanning electron microscopy (SEM) and atomic force microscopy (AFM) were created a scratch line, which provides the heterogeneous nucleation for crystallization and the defined areas for studying crystallization. The SEM and AFM samples were prepared as follows: a newly coated film was first scratched once with a razor blade to create the scratch line after drying in the air for 15 min to evaporate solvent and then put immediately into the crystallization chamber to crystallize for a given time. As expected, the crystallization started from the scratch line. Optical microscopy revealed that the crystallization along the scratch line was not a direct result of scratching, and the scratch line acted only as a surface defect to nucleate polymer chains.[19] To prepare the samples for measurements by grazing incidence reflection infrared (GIR-IR) spectroscopy, the newly coated films were directly put into the crystallization chamber to crystallize for a given time without scratching after they had been dried in the air for 15 min. SEM verified that the crystallization in nonscratched films started from other surface defects on the substrate, such as dust particles or substrate defects.

Crystallization in a vacuum was performed in the SEM sample chamber (ca. 10^{-6} h Pa), and the temperature in the vacuum chamber was estimated by ambient temperatures to be 21−22 °C, as described elsewhere.[19] Crystallization in humidity was performed in a self-made chamber at 21−22 °C. After putting the film samples in the crystallization chamber, the relative humidity (RH) inside the chamber was adjusted with dried and humid nitrogen streams to a given value. During the crystallization process, the humidity and temperature inside the crystallization chamber were monitored by a thermo/hygrometer (Huger Electronics GmbH, Germany). Under careful controls, we got the very stable crystallization conditions in the chamber, where humidity and temperature fluctuated only by $<\pm 1\%$ RH and $<\pm 0.5$ °C, respectively. The crystallization did take place in the humidity chamber, even though the exact time when the crystallization started in the chamber is not known yet. For simplicity, the time when samples were put into the chamber was recorded as the starting time for crystallization. After crystallization for a given time (see Figure legends), the samples were measured immediately with SEM, AFM, and GIR-IR spectroscopy, as described elsewhere.[18,19]

Results

We have previously[19] reported on the crystalline structures in PEO/PMMA blend films crystallized in a vacuum at 21−22 °C. PMMA and PEO form amorphous and metastable blend films as they codeposit from a chloroform solution onto Au surfaces. The gold surface, as prepared in a vacuum, is hydrophilic in nature, but contamination of the gold surface by atmospheric hydrocarbons occurs rapidly when it is exposed to the air, resulting in a hydrophobic surface.[31] Results show that hydrophilic PEO has so weak an interaction with the Au surface that it can be easily removed by solvent,[29] but hydrophobic PMMA can be physically adsorbed onto the Au surface due to the interaction of polar methoxy and carbonyl groups with it.[19,31] Formation of homogeneous PEO/PMMA films is attributed to the anchoring of PEO chains on the Au surface by PMMA.[29] In a vacuum, PEO in the blend films crystallized into fractal-like structures by a DLA process (insets to Figure 1a,c). For details one may refer to our previous work in ref 19.

However, as the blend films crystallized in humidity, the branched structures became much wider than the fractal-like ones formed in a vacuum (Figure 1a,c) and resemble the structure referred to as dense branching morphology (DBM) that is characterized by a stable circular envelope modulated by leading branch tips.[32] DBM structure has been observed by others in experiments on viscous fingering,[33] fluid flow in Hele-Shaw cells,[34,35] electrodeposition,[36] and lipid crystallization.[37] The formation of DBM-like structures was also observed in the crystallization of ultrathin PEO films, as a result of the reduction in polymer concentration in the diffusion filed.[18] The DBM-like structures in the present study resulted reasonably from PEO crystallization in PEO/PMMA films by a DLA process. As PMMA content increased, the DBM-like branches became shorter in length and narrower in width (Figure 1). The thickness of these branches changed with PMMA content, that is, 8 ± 1 nm in 90/10 film (Figure 1b), 10 ± 1 nm in 75/25 film (Figure 1d), and 13 ± 1 nm in 64/40 film (Figure 1f). These values, particularly in 90/10 and 75/25 films, are much higher than those of the branches formed in the corresponding films crystallized in a vacuum (i.e., 4 ± 1 nm in 90/10 film, 6 ± 1 nm in 75/25 film, and 10 ± 1 nm in 60/40 film).[19]

Obviously, changing the crystallization condition from vacuum to humidity brings forth a remarkable transition of crystal growth. The sharp structural transition is clearly shown in Figure 2. As the films crystallized successively in a vacuum and humidity, two kinds of structures were involved, DBM-like fronts and fractal-like branches behind the fronts. The thickness of the DBM-like broad fronts was 8 ± 1 nm in 90/10 film and 10 ± 1 nm in 75/25 film, while that of the fractal-like branches was 5 ± 1 nm in 90/10 film and 6 ± 1 nm in 75/25 film. The DBM-like fronts were undoubtedly related to the crystallization in humidity. With regard to the dimensions of the branches, it is reasonable that the fractal-like branches formed originally in a vacuum. As compared to the crystallization proceeded only in a vacuum, the small increase in the thickness and width of the fractal-like branches after exposure to humidity is attributed to the rearrangement of the crystallized chains during the successive crystallization in humidity. Note, a sharp structural transition, looking similar to Figure 2, was previously observed in the crystallization of PEO in a water-assisted diffusion,[18] which is attributed to the decrease in polymer concentration in the diffusion field. But the origin of the structural transition

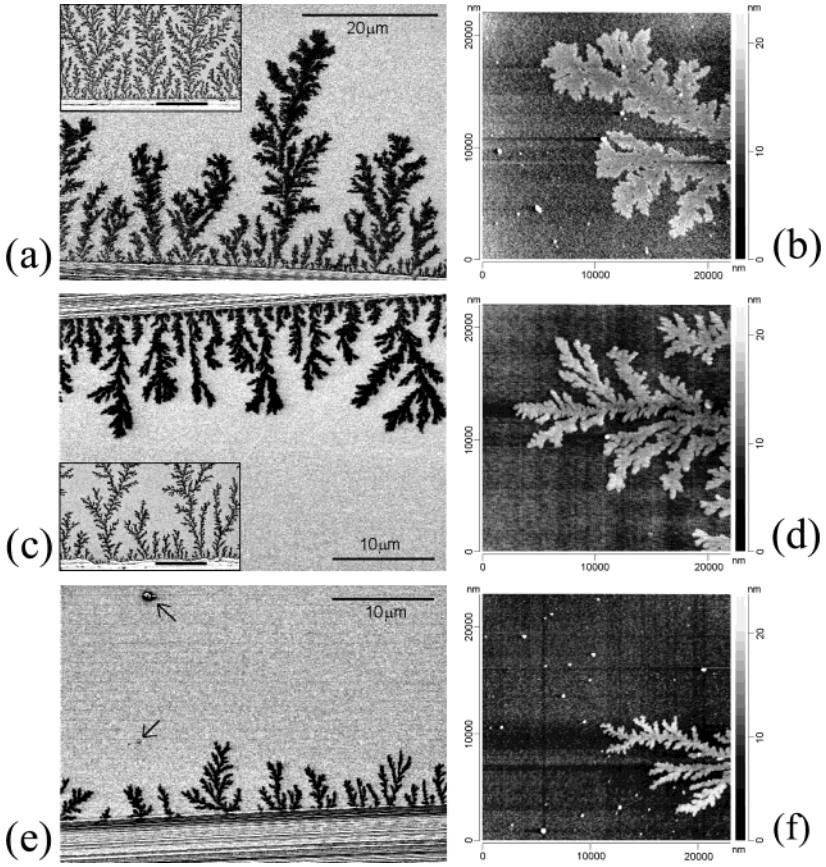

Figure 1. Low-voltage SEM (a, c, e) and noncontact AFM (b, d, f) images of the branched structures resulted from ultrathin PEO/PMMA films crystallized in humidity (22 °C, 47% RH, 23 h). The images correspond to the films with PEO/PMMA weight ratio of (a, b) 90/10 (D = 2.3 nm), (c, d) 75/25 (D = 2.1 nm), and (e, f) 60/40 (D = 2.5 nm). The insets to images (a) and (c) are the structures obtained in the corresponding films in a vacuum (10^{-6} h Pa, 18 h), where the scaling bars equal to 5 μm.

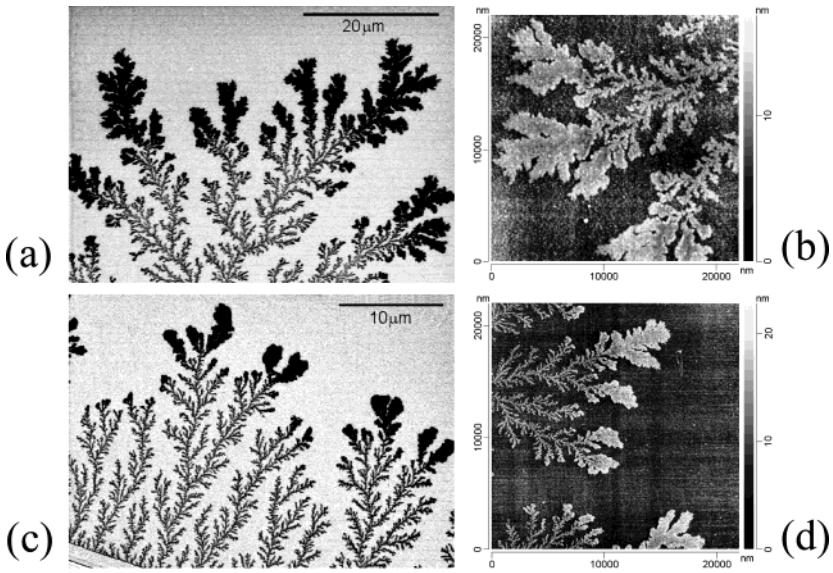

Figure 2. Low-voltage SEM (a, c) and noncontact AFM (b, d) images of the branched structures resulted from ultrathin (a, b) 90/10 film (D = 2.3 nm) crystallized in a vacuum (10^{-6} h Pa, 18 h) and humidity (22 °C, 48% RH, 19 h) and (c, d) 75/25 film (D = 2.2 nm) crystallized in a vacuum (10^{-6} h Pa, 17 h,) and humidity (21 °C, 47% RH, 23 h).

in the present study is different from the previous case (refer to later discussion).

The GIR-IR spectra of the films crystallized in different conditions are shown in Figure 3, where the transmission spectra of PEO in bulk state are also presented for comparison. Detailed assignments of IR vibrations of PEO[8,29,38] and PMMA[31] have been described by others. Compared to the isotropic spectrum of bulk PEO (trace a), the 90/10 film crystallized in humidity (trace b) only exhibits intensively the bands with transition dipole moments parallel (||) to PEO chain axis (1342, 1242, 1107 and 963 cm^{-1}), as is same to its crystallization in a vacuum.[19] In the spectrum of the 75/25 film crystallized successively in a vacuum and humidity (trace c), the vibrations of || bands are clearly exhibited, while they are much weaker than the 90/10

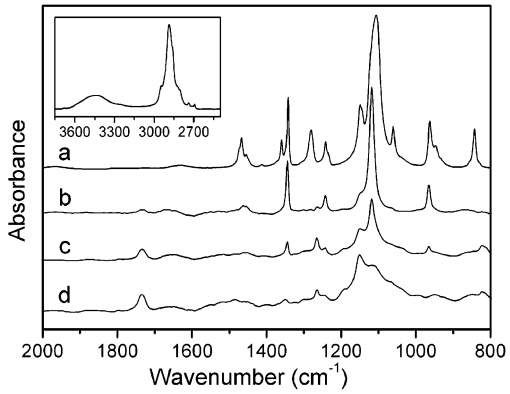

Figure 3. Transmission FT-IR spectrum of PEO in bulk state (a) and GIR-IR spectra of the ultrathin PEO/PMMA films crystallized in different conditions, that is, (b) 90/10 film (D = 2.3 nm) in humidity (22 °C, 48% RH, 20 h), (c) 75/25 film (D = 2.2 nm) successively in a vacuum (10^{-6} h Pa, 17 h) and humidity (21 °C 45% RH, 17 h), and (d) 75/25 film (D = 2.1 nm) in humidity (22 °C, 48% RH, 20 h). The inset shows the IR vibrations of the bulk PEO at high wavenumbers, where the peak at around 3450 cm^{-1} indicates the formation of a hydrogen bond in the solid state (ref 43). The transmission spectrum of PEO in bulk state was recorded in a vacuum at a resolution of 2 cm^{-1} and 32 scans on the same IR spectrometer (IFS66V/S, Bruker Co.) as in GIR-IR measurements, and the bulk sample was made in KBr pellets without any prior treatments of PEO before measurements.

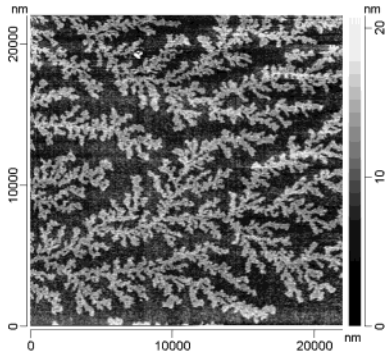

Figure 4. A noncontact AFM image of the fractal-like structures formed in ultrathin PEO film in humidity (22 °C, 55% RH, 17 h). The film was dip-coated from a PEO solution in chloroform (1 mg/mL) and 2.6 nm thick. Comparing the present structure to that formed in a vacuum (Figure 4a in ref 19) shows that almost no remarkable influence of humidity is imposed on PEO crystallization when without PMMA in the crystallization system.

case. But as the 75/25 film crystallized in humidity (trace d), the crystalline signal at 1342 cm^{-1} is very weak, and the vibrations of the || band at 963 cm^{-1} is not remarkable. Because no vibrations of PEO bands with transition dipole moments perpendicular to PEO chain axis[8,29,38] are evident, it is concluded that the PEO chains in the PEO/PMMA films having a history of humidity crystallization orient normal to the substrate surface because in GIR-IR measurements only the bands with transition dipole moment components normal to the substrate surface can be observed.

Discussion

1. Film Reconstruction. To reveal the humidity effect on the crystalline structure, crystallization of PEO film (ca. 3 nm thick) in humidity was carried out, as shown in Figure 4. In humidity the PEO film crystallized into a fractal-like structure, and the crystal lamellae had a thickness of 8 ± 1 nm, as is very similar to its crystallization in a vacuum (Figure 4a in ref 19). Except for a small increase in the width of crystal lamellae in humidity, for which explanation will be given in a later paragraph, almost no influence of humidity on PEO crystallization is remarkable when PMMA is absent from the crystallization system. Therefore, the great changes in the crystalline structures of the blend films during the crystallization in a vacuum and humidity should be related to the film structures under these crystallization conditions.

Known from Figure 1, in humidity the crystals grew only in the close vicinity of the scratch line, leaving a large structureless area in front of the branches. While the possibility to find other surface defects in this structureless area was high as marked by the arrows (Figure 1e), no branches nucleated by these defects were observed in experiments. However, after vacuum crystallization the structureless areas still consists of amorphous PMMA and PEO, and the PEO can be further crystallized if there are other surface defects.[19] Evidently, in humidity PEO chains dewetted to the scratch line to crystallize, and there was no crystallizable PEO in the structureless area ahead of the DBM-like branches.

The dewetting phenomenon on substrate in humidity was also reported in ultrathin blend films ($D \approx 85$ nm) of deuterated polystyrene (dPS) and poly(vinyl methyl ether) (PVME), where PVME is a moisture-sensitive polymer,[39] but how it proceeded is unclear. As shown in a series of PEO/PMMA blend films crystallized in a vacuum,[19] the GIR-IR band at 1150 cm^{-1} is sensitive to PMMA content, but the band at 1107 cm^{-1} is mainly related to PEO, and 75/25 film and those with PMMA content <40% exhibit a weaker signal of PMMA at 1150 cm^{-1} than PEO at 1107 cm^{-1}, but at PMMA content ≥40% the signal at 1150 cm^{-1} becomes stronger than that at 1107 cm^{-1} and the intensity ratio of I_{1150}/I_{1107} in 50/50 film is 1.17. However, after crystallization in humidity, 75/25 film exhibits a stronger band at 1150 cm^{-1} than at 1107 cm^{-1} (Figure 3, trace d), with an intensity ratio of $I_{1150}/I_{1107} \approx 1.26$ which is much larger than the intensity ratio of 1.17 obtained in the 50/50 film crystallized in a vacuum. Since after crystallization in a vacuum the films with PMMA content ≥40% remain mainly amorphous where the distribution of PMMA are homogeneous,[19] the GIR-IR spectra of them can be used as a reference for evaluating the PMMA distribution in the 75/25 film crystallized in humidity. It is, therefore, derived that PMMA content in the GIR-IR scanned area of the 75/25 film crystallized in humidity was enhanced to a value higher than 50%. The increase in PMMA content after exposure to humidity infers that PMMA remained unmoved on the Au surface during PEO dewetting, which may be due to the interaction between PMMA and substrate.

On the basis of the SEM and GIR-IR results, a reconstruction of the blend films in humidity is turned out, which makes hydrophilic PEO chains segregate to the free film interface (air/polymer),[40] as shown in Figure 5. Therefore, an original PEO/PMMA blend film actually turns in humidity into a "nonblend" one before or during crystallization, and the PEO chains diffuse to crystallize on PMMA layer. After water etching of the 90/10 and 75/25 films crystallized in humidity to remove the PEO crystals, no depth profiles were detected by AFM at the locations where PEO crystal branches grew. This additionally supports, to a certain extent, that the DBM-like branches lie on PMMA layer.

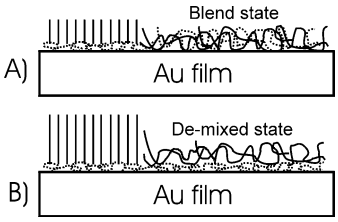

Figure 5. Schematic illustration of chain ordering processes in PEO/PMMA films in a vacuum (A) and humidity (B). The dotted lines represent PMMA chains and the solid ones PEO chains. Polymer chains in crystal lamellae come from the amorphous PEO ahead of them. In the blend state (A), the crystal growth is dominated by either the kinetic effect or the surface tension effect at crystal growth fronts depending on the film composition; that is, it is by the kinetic effect when PMMA content is low but turns to a weak surface tension effect upon increasing PMMA content. However, the crystal growth is dominated by a strong surface tension effect at crystal growth fronts in the demixed state (B) because of a high chain mobility.

On the other hand, in the blend state (Figure 5A) the width of crystal lamellae will be determined by two factors: one is the kinetics of the chain deposition rate at crystal growth fronts, and another is the PMMA phases that are excluded laterally from the crystal phases to beside the lamellae. Results[19] have shown that the width of the crystal lamellae is mainly related to the later factor because the existence of the excluded PMMA phases can prevent the chain deposition at the side faces of the lamellae. Under the demixed situation (Figure 5B), however, no or very few PMMA chains will be excluded from crystal phases to the side faces of crystal lamellae, which opens the possibility for sticking PEO chains to occupy a favorable location with a low energy at the growth fronts and further to broaden the lamellae.[18] This is confirmed by the result that the crystal lamellae formed in humidity are much wider than those formed in a vacuum (Figures 1 and 2).

2. Characterization of Branched Structures. Since the PEO chains within the crystals take exclusively a conformation with chain axes perpendicular to the substrate surface (Figure 3) and the crystal growth mainly proceeds laterally (Figures 1 and 2), the DBM-like branches are therefor the crystal lamellae viewed flat-on on PMMA layer and the multipacking of crystal lamellae is not the case in these structures. This conclusion is further supported by the result (not documented) that the branches formed in humidity (24 h, 47% RH, 22 °C) in 90/10 film ($D \approx 2-3$ nm) consisting of the PMMA and a shorter PEO (poly(ethylene glycol) standard, from Fluka, $M_w = 1960$, $M_w/M_n = 1.03$) had a thickness of 12 ± 1 nm, which is very comparable to the length L of the fully extended crystalline short PEO chains ($L = 12$ nm) according to $L = (M_n^{PEO}/M_n^{EO}) \times 0.2783$ nm.[21] Therefore, the thickness of the DBM-like branches is a direct measure of the PEO chain folding states in the crystal lamellae (Figure 1), that is, the crystallized PEO chains ($L = 37$ nm) in 90/10, 75/25, and 60/40 films fold 4, 3, and 2 times, respectively.

As PEO/PMMA blend films crystallize in a vacuum, there is a possible discrepancy between the actual and measured thickness values of the crystal lamellae, particularly in the films with a high PMMA content (e.g., ≥40%), due to the excluded PMMA phases segregating laterally beside the lamellae.[19] As PMMA content is low, in 90/10 and 75/25 films for example, the discrepancy should be very small, we can use the crystal lamellae in these films to make a direct comparison between the vacuum and humidity crystallization. On the other hand, the fractal-like lamellae (10 ± 1 nm by AFM) formed in 60/40 film in a vacuum (Figures 1d and 4d in ref 19) should be actually thinner than the DBM-like ones (13 ± 1 nm) formed as it crystallized in humidity (Figure 1e,f), because during the crystallization in a vacuum PMMA phases may be excluded to beneath and beside the lamellae and the thickness of PMMA layer beside a lamella should be less than 3 nm, the value of maximum film thickness. It is clear that, within the tested composition range (10−40% PMMA), the DBM-like lamellae are thicker, but much thicker when PMMA content is rather low, than the fractal-like ones, and the crystallization in humidity is (much) closer to equilibrium.[16,17]

3. Transition of Crystal Growth. 3.1. Kinetic and Surface Tension Effects in Crystallization by the DLA Process. Aggregate formation by nonequilibrium growth exists commonly in solidification and crystallization processes. A model referred to as DLA was introduced by Witten and Sander[22] to describe theoretically the aggregate formation in a diffusion-controlled system, where a diffusing particle sticks irreversibly to the surface of a growing aggregate during its random walking process, resulting in fractal aggregates. Because a newly deposited particle does not subsequently move around on the surface of the growing aggregate in an attempt to minimize its energy, DLA is a nonequilibrium and kinetically driven process. For a convenient discussion, we refer here the original DLA process to as one with kinetic effect. However, as the microscopic effect of surface tension that favors the minimized interface area of a growing aggregate is considered in the DLA process via phenomenological rules for sticking probability of the walkers to the aggregate,[41] that is, the growth rate or the sticking probability is reduced at the places with a large interface curvature, a compact aggregate is turned out, which is referred to as DBM.[32,35] As the results of the surface tension effect, the position of a newly deposited particle is relaxed to one with the lowest potential energy and the largest number of occupied nearest neighbors, and the tip of the growing aggregate becomes smooth and rounded. These processes lead to broad aggregates.[41,42] The DLA morphology is, therefore, viewed as the limit of DBM for vanishing effective surface tension.[35]

In fact, the surface tension effect and kinetic effect are two competitive factors in influencing the structures of aggregates formed by the diffusion-controlled process. While the kinetic effect will lead to the structures in a state far away from equilibrium, the surface tension effect will make the structures close to equilibrium. When describing the nonequilibrium crystallization in ultrathin polymer films by the DLA process, where a diffusing chain is regarded as a walking particle, the kinetic and surface tension effects should be taken into consideration. Previous results have shown that the surface tension effect can be initiated by the reduction in polymer concentration in the diffusion field[18] and by decreasing film thickness.[11] Actually, that elevating T_c leads to wider and thicker PEO crystal lamellae[15−17] can also be attributed to the enhanced surface tension effect at elevated temperatures (refer to the Introduction). The experimental and theoretical results indicate that the crystal lamellae will be thickened and broadened as the crystal growth in the DLA process changes from being

dominated by kinetic effect to one dominated by the surface tension effect, and factors that lower the chain deposition rate at crystal growth fronts favor the surface tension effect.

3.2. Transition from Fractal- to DBM-like Structures in Blend Films. Comparison between the PEO film crystallization in humidity (Figure 4) and in a vacuum (Figure 4a in ref 19) shows that the humidity imposes a faint influence to increase the lamellae width, which can be understood by the mobility of PEO chains on the substrate surface. Since the PEO chains used in the present study are terminated by OH at both ends, the coupling of end groups mainly by a hydrogen bond in the solid state, which is indicated by the peak at around 3450 cm^{-1} in the transmission FT-IR spectrum of the bulk PEO (inset to Figure 3),[43] will result in actually longer PEO chains, inevitably leading to the reduced mobility of PEO chains as compared to that of the original and shorter PEO chains. As exposed to humidity, water phase condensed on a substrate surface will impose two effects to increase the mobility of PEO chains: one is water molecules will cleave the existing hydrogen bond between two PEO chains by forming new hydrogen bond with the ether oxygen of PEO,[44] and another is the dissolution effect of condensed water on PEO chains. The small increase in the width of crystal lamellae in humidity crystallization can be accounted for by the relatively larger diffusion path of chains[16,17] due to the enhanced chain mobility by the condensed water. Obviously, the water influence is not sufficiently strong to change the lamellae thickness in the PEO film.

The different crystal structures in the blend films crystallized in a vacuum and humidity have been demonstrated to be related to the film structures by our SEM, AFM, and GIR-IR results at the beginning of the Discussion section. As shown in the vacuum crystallization of PEO/PMMA blend films (Figure 5A), crystal growth depends on the film composition;[19] that is, the crystal growth process is dominated by kinetic effect as PMMA content is rather low (e.g., in 90/10 and 75/25 films) and the resultant crystals are far away from equilibrium, but upon increasing PMMA content to ≥40% the strong retardation of PMMA makes a lowered chain deposition rate at crystal growth fronts and an easier relaxation of the deposited chains toward a state of minimized energy, resulting in the crystal growth process dominated by the surface tension effect. Note, we did not observe in the vacuum crystallization the change in lamellar width accompanying the thickness increase as the surface tension effect is enhanced by increasing PMMA, which is attributed to the confinement of the lamellar width imposed by PMMA phases excluded laterally from the crystals.[19]

With respect to the reconstruction of film in humidity (Figure 5B), as PEO chains segregate at the free interface the mobility of them is remarkably enhanced.[45] The demixed PEO chains have a high ability to diffuse around before getting trapped in crystal phases, and the existence of water phase condensed on the film surface will inevitably strengthen this diffusion process. The high mobility of PEO chains will increase the effective diffusion path of them during crystallization process, as is similar to the effect of elevating T_c.[16,17] Hence, the crystal growth in humidity is reasonably dominated by a strong surface tension effect due to a lowered deposition rate of the demixed PEO chains at crystal growth fronts as a result of the elongated effective diffusion path.

The transition of crystal structures when crystallization changes from in a vacuum to in humidity can be explained by the chain deposition kinetics. As PMMA content is low (e.g., ≤25%), completely different crystal growth processes are the origin for the phenomenon that crystal lamellae formed in humidity are much higher and wider than those formed in a vacuum (Figures 1 and 2); that is, the crystal growth is dominated by the kinetic effect in a vacuum but by the surface tension effect in humidity. However, as PMMA content is high (e.g., ≥40%), the situation becomes a bit complex in that the crystal growth process in a vacuum is also dominated by the surface tension effect due to the retarded chain mobility by PMMA.[19] One should notice that the surface tension effect in the blend state (vacuum crystallization) originates from the retardation of PMMA, but in the demixed state (humidity crystallization) from the elongated diffusion path. As indicated by the result that the crystal lamellae in 60/40 film are thicker and wider in humidity crystallization (Figure 1e,f) than in a vacuum crystallization (Figures 1d and 4d in ref 19), the surface tension effect caused by the elongated diffusion path is stronger. Therefore, the transition from fractal- to DBM-like structures is attributed to the change in the crystal growth from one dominated by kinetic effect (i.e., films with PMMA ≤ 25%) or one dominated by a weak surface tension effect (i.e., films with PMMA ≥ 40%) in a vacuum to a growth process dominated by a strong surface tension effect in humidity, as a result of the different polymer states in a vacuum and humidity.

4. Compositional Dependence of DBM-like Structures. As illustrated in Figure 5, the deposition kinetics of polymer chains at crystal growth fronts in humidity should relate to two processes. The first is the demixing process between PEO and PMMA, and the second is the transportation of the demixed PEO chains to the crystal growth fronts on PMMA layer. Because in such thin films the entanglements among demixed PEO chains will not come to influence their diffusion property,[46] the diffusion coefficients of the PEO chains on PMMA layer should be same in the films with different PMMA contents under the same temperature and humidity conditions. Thus, the chain deposition kinetics at growth fronts is mainly affected by the demixing process. Upon increasing PMMA content, it becomes more difficult for PEO to demix from the blend state because of a more rigid film and a stronger anchoring effect of PMMA on PEO;[29] then it will finally take a longer time for PEO chains to diffuse to crystal growth fronts, resulting in a lower chain deposition rate (i.e., a stronger surface tension effect) at the crystal growth fronts and a longer time for the deposited chains to relax to a state closer to equilibrium. As expected, the thickness of crystal lamellae increases with increasing PMMA content (Figure 1).

On the other hand, as expected from the simulation of the surface tension effect on aggregate growth,[41,42] the stronger surface tension effect generated with increasing PMMA content would lead to wider crystal lamellae. But, our results show that the width of the lamellae reduces with increasing PMMA (Figure 1). We do not think our results contradict the theoretical expectation. Apart from the kinetics of chain deposition, another factor influencing the width of crystal lamellae

is the population of crystallizable PEO chains, which should be taken into consideration in discussing the lamellar width in these different films. The original PEO/PMMA blend film on substrate is actually a reservoir to supply PEO chains on the PMMA layer. As PMMA content increases, the population of the demixed PEO chains is reduced due to a lower PEO fraction in the blend and a stronger retardation effect of PMMA on the demixing. This inevitably limits the lamellar growth in two dimensions, leading to a smaller width and length of crystal lamellae. This argument is also not contradictory to our previous result that the reduction in polymer concentration in the diffusion field will lead to wider, and thicker as well, lamellae.[18] It should be noted that our previous conclusion was made in the same diffusion field. In fact, one can notice that in the same sample in the present study (Figure 1a,c) the fronts of the branches are somewhat wider than the parts behind the fronts, which is consistent with our previous result.

The PEO and 90/10 films had a relatively comparable PEO content, but the humidity imposed a very faint effect on the crystalline morphology in PEO film but a great one in the blend film. Since the existence of PMMA in this blend film would accelerate rather than retard the demixing between PEO and PMMA,[19] the greater effect of humidity on the crystal structures in 90/10 film than in PEO film seems to be strongly related to the appearance of the interface between PEO and PMMA layers in the former case (Figure 5B), even though the interaction between PEO and PMMA has been demonstrated to be very weak.[47] How the PEO−PMMA interface influences the transportation of PEO chains on the PMMA layer is in progress.

Conclusion

This study presents the transition of crystal growth during nonequilibrium crystallization in ultrathin films ($D = 2-3$ nm) consisting of PEO and PMMA as a result of changing the PEO from a blend state to a demixed one. Crystal growth in ultrathin polymer films is dominated by two competitive factors at the crystal growth fronts, the kinetic and surface tension effects. In a vacuum crystallization, PEO crystallizes from a state mixed with PMMA into fractal-like structures; the crystal growth is dominated by the kinetic effect as PMMA content is rather low (e.g., 90/10 and 75/25 films) but turns gradually to by the surface tension effect upon increasing PMMA content.[19] However, a blend film changes in humidity into a demixed structure with PEO segregating on PMMA layer during/before crystallization. The demixed PEO chains crystallize into DMB-like structures on the PMMA layer, where the crystal growth is dominated by the surface tension effect. As crystallization condition changes from vacuum to humidity, the crystal growth is consequently changed from one dominated by the kinetic effect or by a weak surface tension effect to a growth process dominated by a strong surface tension effect, as a result of the alteration of polymer states in the films. The transition of crystal growth habits leads to the different crystal structures observed. Our results clearly indicate that far from equilibrium it is the kinetic effect that stabilizes the growing front, whereas near equilibrium the surface tension effect is dominant, as agrees well with the dendritic growth.[34]

Acknowledgment. We acknowledge the DFG for supporting this work (priority program "Wetting and Structure Formation at Surfaces"). M. Wang acknowledges the Alexander von Humboldt Foundation for a research fellowship. We also acknowledge the referees and the editor involved for their generous advice on revision.

References and Notes

(1) Tseng, K. C.; Turro, N. J.; Durning, C. J. *Phys. Rev. E* **2000**, *61*, 1800−1811.
(2) (a) Frank, C. W.; Rao, V.; Despotopoulou, M. M.; Pease, R. F. W.; Hinsberg, W. D.; Miller, R. D.; Rabolt, J. F. *Science* **1996**, *273*, 912−915. (b) Despotopoulou, M. M.; Frank, C. W.; Miller, R. D.; Rabolt, J. F. *Macromolecules* **1996**, *29*, 5797−5804.
(3) Despotopoulou, M. M.; Miller, R. D.; Rabolt, J. F.; Frank, C. W. *J. Polym. Sci., Part B: Polym. Phys.* **1996**, *34*, 2335−2349.
(4) Bartczak, Z.; Argon, A. S.; Cohen, R. E.; Kowalewski, T. *Polymer* **1999**, *40*, 2367−2380.
(5) Reiter, G. *Macromolecules* **1994**, *27*, 3046−3052.
(6) (a) Fryer, D. S.; Nealey, P. F.; de Pablo, J. J. *Macromolecules* **2000**, *33*, 6439−6477. (b) Torres, J. A.; Nealey, P. F.; de Pablo, J. J. *Phys. Rev. Lett.* **2000**, *85*, 3221−3224.
(7) Schönherr, H.; Bailey, L. E.; Frank, C. W. *Langmuir* **2002**, *18*, 490−498.
(8) Schönherr, H.; Frank, C. W. *Macromolecules* **2003**, *36*, 1188−1198.
(9) Schönherr, H.; Frank, C. W. *Macromolecules* **2003**, *36*, 1199−1208.
(10) Dalnoki-Veress, K.; Forrest, J. A.; Massa, M. V.; Pratt, A.; Williams, A. *J. Polym. Sci., Part B: Polym. Phys.* **2001**, *39*, 2615−2621.
(11) Taguchi, K.; Miyaji, H.; Izumi, K.; Hoshino, A.; Miyamoto, Y.; Kokawa, R. *J. Macromol. Sci., Part B: Phys.* **2002**, *B41*, 1033−1042.
(12) Tauchi, K.; Miyaji, H.; Izumi, K.; Hoshino, A.; Miyamoto, Y.; Kokawa, R. *Polymer* **2001**, *42*, 7443−7447.
(13) Sakai, Y.; Imai, M.; Kaji, K.; Tsuji, M. *J. Cryst. Growth* **1999**, *203*, 244−254.
(14) Sakai, Y.; Imai, M.; Kaji, K.; Tsuji, M. *Macromolecules* **1996**, *29*, 8830−8834.
(15) Reiter, G.; Sommer, J.-U. *Phys. Rev. Lett.* **1998**, *80*, 3771−3774.
(16) Reiter, G.; Sommer, J.-U. *J. Chem. Phys.* **2000**, *112*, 4376−4383.
(17) Sommer, J.-U.; Reiter, G. *J. Chem. Phys.* **2000**, *112*, 4384−4393.
(18) Wang, M.; Braun, H.-G.; Meyer, E. *Macromol. Rapid Commun.* **2002**, *23*, 853−858.
(19) Wang, M.; Braun, H.-G.; Meyer, E. *Polymer* **2003**, *44*, 5015−5021.
(20) (a) Kovacs, A. J.; Gonthier, A.; Straupe, C. *J. Polym. Sci., Polym. Symp.* **1975**, *50*, 283−325. (b) Kovacs, A. J.; Straupe, C.; Gonthier, A. *J. Polym. Sci., Polym. Symp.* **1977**, *59*, 31−54.
(21) Kovacs, A. J.; Straupe, C. *J. Cryst. Growth* **1980**, *48*, 210−226.
(22) (a) Witten, T. A.; Sander, L. M. *Phys. Rev. Lett.* **1981**, *47*, 1400−1403. (b) Sander, L. M. *Nature (London)* **1986**, *322*, 789−793.
(23) Sawamura, S.; Miyaji, H. Izumi, K.; Sutton, S. J.; Miyamoto, Y. *J. Phys. Soc. Jpn.* **1998**, *67*, 3338−3341.
(24) (a) Bassett, B. C. *Principles of Polymer Morphology*; Cambridge University Press: Cambridge, 1981. (b) Strobl, G. *The Physics of Polymers*; Springer-Verlag: Berlin, 1996.
(25) For the detailed discussions of polymer crystallization one can refer to some review articles: (a) Armitstead, K.; Goldbeck-Wood, G. *Adv. Polym. Sci.* **1992**, *100*, 183−312. (b) Hoffman, J. D.; Miller, R. L. *Polymer* **1997**, *38*, 3151−3212. (c) Ungar, G.; Zeng, X. *Chem. Rev.* **2001**, *101*, 4157−4188. (d) Phillips, P. J. *Rep. Prog. Phys.* **1990**, *53*, 549−604. (e) Geil, P. H. *Polymer* **2000**, *41*, 8983−9001. (e) Keller, A. *Rep. Prog. Phys.* **1968**, *31*, 623−704.
(26) (a) Barnes, W. J.; Luetzel, W. G.; Price, F. P. *J. Phys. Chem.* **1961**, *65*, 1742−1748. (b) Pearce, R.; Vancso, G. J. *Macromolecules* **1997**, *30*, 5843−5848.
(27) Hobbs, J. K.; McMaster, T. J.; Miles, M. J.; Barham, P. J. *Polymer* **1998**, *39*, 2437−2446.

(28) Lisowski, M. S.; Liu, Q.; Cho, J.; Runt, J.; Yeh, F.; Hsiao, B. S. *Macromolecules* **2000**, *33*, 4842−4849 and references therein.
(29) Hoffmann, C. L.; Rabolt, J. F. *Macromolecules* **1996**, *29*, 2543−2547.
(30) Lin, E. K.; Kolb, R.; Satija, S. K.; Wu, W. *Macromolecules* **1999**, *32*, 3753−3757.
(31) Lenk, T. J.; Hallmark, V. M.; Rabolt, J. F.; Häussling, L.; Ringsdorf, H. *Macromolecules* **1993**, *26*, 1230−1237.
(32) Ben-Jacob, E. *Contemp. Phys.* **1993**, *34*, 247−273.
(33) Arnéodo, A.; Couder, Y.; Grasseau, G.; Kakim, V.; Rabaud, M. *Phys. Rev. Lett.* **1989**, *63*, 984−987.
(34) Ben-Jacob, E.; Garik, P.; Mueller, T.; Grier, D. *Phys. Rev. A* **1988**, *38*, 1370−1380.
(35) Ben-Jacob, E.; Deutscher, G.; Garik, P.; Goldenfeld, N. D.; Lareah, Y. *Phys. Rev. Lett.* **1986**, *57*, 1903−1906.
(36) (a) Sawada, Y.; Dougherty, A.; Gollub, J. P. *Phys. Rev. Lett.* **1986**, *56*, 1260−1263. (b) Grier, D.; Ben-Jacob, E.; Clarke, R.; Sander, L. M. *Phys. Rev. Lett.* **1986**, *56*, 1264−1267.
(37) Miller, A.; Knoll, W.; Möhwald, H. *Phys. Rev. Lett.* **1986**, *56*, 2633−2636.
(38) Yoshihara, T.; Tadokoro, H.; Murahashi, S. *J. Chem. Phys.* **1964**, *41*, 2902−2911.
(39) Karim, A.; Slawecki, T. M.; Kumar, S. K.; Douglas, J. F.; Satija, S. K.; Han, C. C.; Russell, T. P.; Liu, Y.; Overney, R.; Sokolov, J.; Rafailovich, M. H. *Macromolecules* **1998**, *31*, 857−862.
(40) Russell, T. P. *Science* **2002**, *297*, 964−967.
(41) (a) Vicsek, T. *Phys. Rev. Lett.* **1984**, *53*, 2281−2284. (b) Vicsek, T. *Phys. Rev. A* **1985**, *32*, 3084−3089.
(42) Barra, F.; Davidovitch, B.; Levermann, A.; Procaccia, I. *Phys. Rev. Lett.* **2001**, *87*, 134501.
(43) Cheng, S. Z. D.; Wu, S. S.; Chen, J.; Zhuo, Q.; Quirk, R. P.; von Meerwall, E. D.; Hsiao, B. S.;Habenschuss, A.; Zschack, P. R. *Macromolecules* **1993**, *26*, 5105−5117.
(44) Kyritsis, A.; Pissis, P. *J. Polym. Sci., Part B: Polym. Phys.* **1997**, *35*, 1545−1560.
(45) Keddie, J. L.; Jones, R. A. L.; Cory, R. A. *Europhys. Lett.* **1994**, *27*, 59−64.
(46) Brown, H. R.; Russell, T. P. *Macromolecules* **1996**, *29*, 798−800.
(47) Rao, G. R.; Castiglioni, C.; Gussoni, M.; Zerbi, G.; Martuscelli, E. *Polymer* **1985**, *26*, 811−820.

MA0355812